Experiments with a self-propelled body submerged in a fluid with a vertical density gradient

By ALLEN H. SCHOOLEY

U.S. Naval Research Laboratory, Washington 25, D.C.†

AND R. W. STEWART

Institute of Oceanography, University of British Columbia, Vancouver 8, B.C.

(Received 2 August 1962)

It is shown that the turbulent wake of a self-propelled body moving in a fluid with a vertical density gradient is considerably different than of the same body moving in a fluid having no density gradient. In the uniform density case, the turbulent mixed fluid behind the body expands into an irregular conical shape. In the case of a density gradient, the initial expansion of the mixed fluid is quickly followed by a collapse in the vertical direction which is accompanied by a further spreading in the horizontal direction. This phenomenon is caused by the force of gravity. The volume of fluid behind the self-propelled body has a more or less constant density due to mixing. Thus, it is forced to seek its own density level in the undisturbed fluid.

The collapsing vertical wake is shown to be an efficient generator of internal waves, many of high order. These manifest themselves in surface movements.

The assumption that the internal waves are damped only by viscosity, not by turbulence, leads to results in general accord with the observations.

Experimental equipment

Figure 1, plate 1, is an over-all picture of the experimental apparatus. The tank is constructed of wood with transparent plastic facings. It is approximately 17·5 cm wide, 33 cm deep, and is 100 cm long at the bottom and 150 cm long at the top. The tank was filled with about 24 l of fluid to a depth of about 12·5 cm. A substantially uniform density gradient was formed by using 12 layers of different mixtures of water and glycerin. The bottom layer contained 22 % glycerin (by volume) which gives a density of about 1·063 g ml. Each succeeding layer had 2 % less glycerin. Thus, the twelfth and top layer was 100 % water. The average over-all density gradient was thus about $5{\cdot}2 \times 10^{-3}$ g ml^{-1} cm^{-1}.

The various layers were introduced into the tank by means of a fountain syringe. In order to minimize mixing during the filling process it was necessary to stop the downward momentum of the liquid and divert it horizontally. This was done by having the syringe nozzle pointed downward towards a thin balsa-wood sheet floating on the surface. Guides were necessary to prevent the sheet from moving out from under the nozzle. After filling, the balsa sheet was care-

† Work done at the Scripps Institution of Oceanography, University of California, La Jolla, California.

fully removed and the tank not used for a few hours to allow a diffusing and blending of the layers to simulate more nearly a uniform gradient.

Figure 2, plate 2, shows a close-up of the self-propelled body in the starting position at the left end of the tank. It consists of a small permanent-magnet-field motor having a diameter of about 2·2 cm. The 1·8 cm diameter plastic propeller is from a toy boat. The over-all length of the self-propelled body is about 4·5 cm. It is held in place by means of a re-formed paper clip hanging from the horizontal guide wire. One of the four supports for the guide is shown in figure 2. It is secured to the bottom of the tank with a rubber suction cup. The guide wire is lacquered black at the starting and stopping positions so that the paper clip will not make contact with the wire at these positions. The energy for the motor is supplied by a single dry cell, one terminal of which is connected to the guide wire, the other to a small flexible wire that trails from the bottom of the motor. The motor circuit is completed through the paper clip. Thus, the motor will not run until pushed off the non-conducting part of the guide wire at the start and will automatically stop at the other end. Launching is accomplished by means of a long straight wire spring, the end of which is shown being held against the left end of the paper-clip support in figure 2. Upon release, the spring moves the motor forward on to the conducting region and it is self-propelled over the centre 50 cm length of the guide wire. The spring launching creates much less acceleration disturbance to the rather small volume of fluid in the tank than occurs if the motor is accelerated by the propeller alone.

Figure 1 shows the 16 mm motion picture camera used in obtaining pictures from which the quantitative data were derived. By means of the 45° mirror, shown in the centre of the tank, it was possible to photograph simultaneously the passage of the self-propelled body from above while it was being photographed directly from the side. A transparent horizontal glass reticle is shown in place just above the water surface and under the mirror.

Experimental results

Figure 3, plate 3, shows the horizontal and vertical profiles of wakes caused by the passage of a self-propelled body through plain water without a density gradient (left three pictures), and also a similar situation with a fluid having a density gradient of $5{\cdot}2 \times 10^{-3}$ g ml^{-1} cm^{-1} (right three pictures). In both cases the propelled body was 7·5 cm below the surface and travelled at about 45 cm/sec. The top two pictures may be considered taken at zero time. The next two pictures were taken 1 sec later, and the bottom two pictures were taken 3 sec after the first ones. The turbulent region behind the model was made visible by dispensing blue liquid food colouring just in front of the propeller. This was done by attaching a glass tube to the body in such a way that its forward motion would force the dye contained in the tube through a nozzle directed to the front of the propeller. The dye was mixed with the proper amount of glycerin to make it slightly more dense than the fluid at the level of the propeller. By making the glass tube slightly bent at the two ends, it was possible to minimize leakage of the dye out of the tube before starting.

Comparison of the top two pictures of figure 3 shows that there is little difference

in the initial growth of the wakes, either horizontally or vertically, regardless of whether there is a density gradient or not. At the end of the first second, as shown in the middle two pictures, the vertical wake in the uniform-density case is wider than in the density-gradient case. This is even more evident in the bottom two pictures that were taken 3 sec after the first ones.

The build-up and subsequent collapse of the wake in the vertical direction when there is a density gradient is particularly interesting. The build-up is due to the expanding region of turbulent fluid which has been given momentum by the

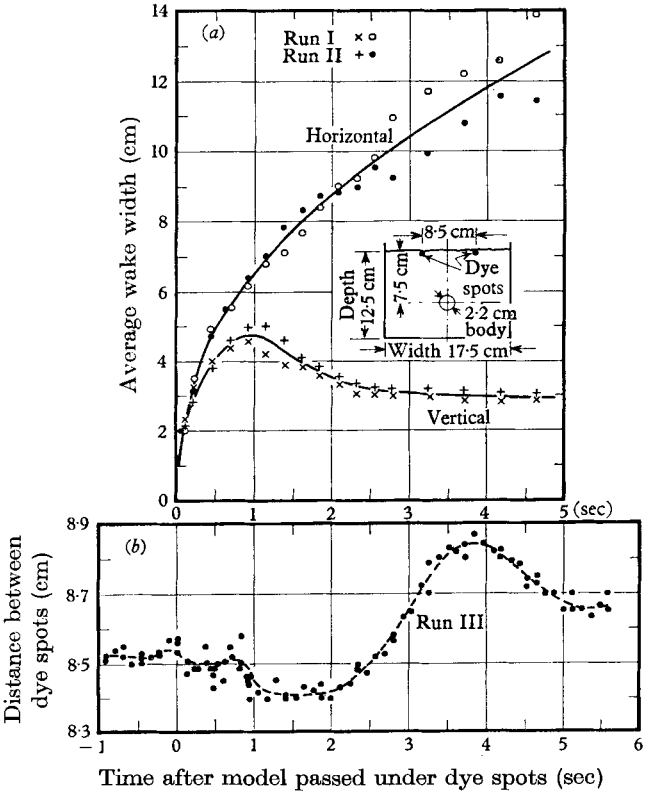

FIGURE 4. (*a*) Horizontal and vertical average wake widths versus time after body passes through a fluid with a vertical density gradient; runs I and II. (*b*) Horizontal distance between two dye spots 5 mm below fluid surface and initially placed about 4·25 cm on each side of the centre line; run III.

passage of the submerged body and the action of its propeller. The turbulent motion also mixes the 'tube' of fluid in the wake so that it attains a more or less uniform density which is the average density of the fluid from which it was mixed. However, a tube of constant-density fluid is not stable in a density gradient. Gravity causes such a tube of fluid to tend to seek its own density level in the surrounding fluid. In so doing, the tube is flattened in the vertical direction and extended horizontally. In a perfect infinite fluid with a vertical density gradient, the initial tube of mixed fluid would ultimately become infinitesimally thin vertically and infinitely wide horizontally. Practically, it is not possible to attain the idealized situation. In the case of the experiments described herein the

greatest limitation was the size of the tank compared to the size of the self-propelled body. The width of the tank was only about eight times, and the depth of the fluid only about five times, the body diameter. If these ratios had been greater the final vertical collapse shown in figure 3 (*f*) would have been more pronounced and the spreading of the horizontal wake would have been easier to see.

Figure 4 (*a*) presents quantitative data showing, for two runs, average wake width versus time for a fluid with a vertical density gradient. Zero time was counted when the plane of the propeller of the self-propelled body cut the vertical and horizontal lines where measurements were made. The horizontal width is continuing to increase at the end of 5 sec and has spread to about three-quarters of the

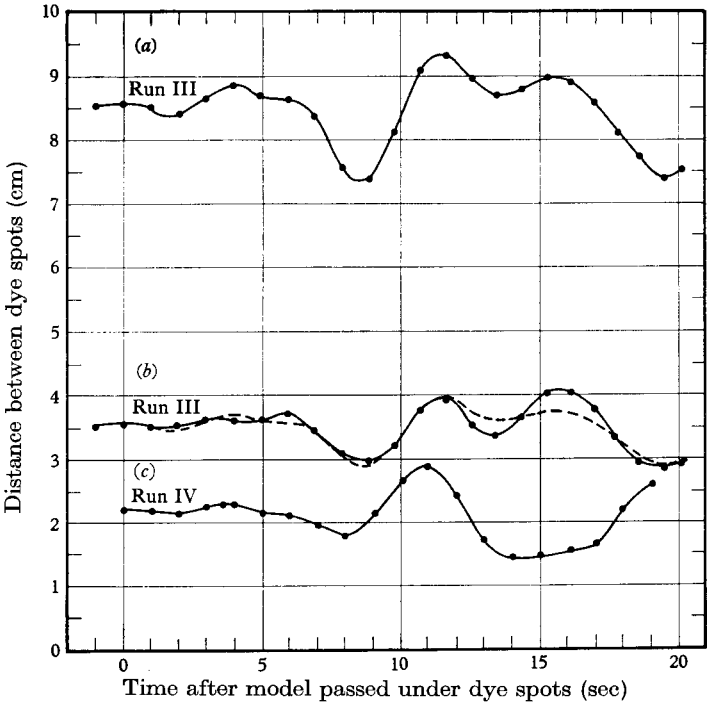

FIGURE 5. (*a*) Same as figure 4 (*b*) except longer time scale; run III. (*b*) Solid curve represents horizontal distance between dye spots initially 1·75 cm on each side of the centre line; run III. Dashed curve is same as figure 5 (*a*) except that ordinate is multiplied by 0·59. (*c*) Horizontal distance between dye spots, one initially 0·5 cm from the centre line, the other 1·7 cm on the other side of the centre line; run IV.

tank width. The vertical width increases to a peak at about 1 sec and the rate of increase is less than for the horizontal wake. After 1 sec the vertical wake starts to collapse and continues until about 2·5 sec.

The vertical collapse of the mixed wake behind a self-propelled body moving in a fluid having a density gradient must of necessity cause readjustments in the surrounding fluid. It would be expected that the vertical collapse would cause convergence at the surface, perpendicular to the wake, in much the same way that convergence at the surface is caused by internal gravity waves. As will be seen below, the wake collapse also excites internal waves that cause a series of convergences and divergences until the internal waves are damped out.

Figure 5 shows the results of measurements of readjustments due to wake collapse. The ordinate is the horizontal distance between two dye spots which were placed about 5 mm below the surface, on a line perpendicular to the path of the submerged body. The origin of the time scale is the same as is used in figure 4.

In figure 5 (*a*) is shown the separation of two spots, originally about 4·25 cm on either side of the centre line in run III. Figure 5 (*b*) is also from run III, but the spots were only 1·75 cm from the centre line. The dashed line in figure 5 (*b*) will be discussed below in the section on theory.

Figure 5 (*c*) concerns run IV. In this case one spot was initially 0·5 cm from the centre line, the other 1·8 cm on the other side. As will be seen below, the motions shown in figure 5 are associated with internal waves.

Figure 4 (*b*) is an enlarged version of the data shown in figure 5 (*a*), to emphasize the early behaviour. The small divergence just before zero time is interesting. It is so small that it is almost unobservable in the 'noise' of measurement error. It is possible that this divergence and the very small convergence at about $\frac{1}{2}$ sec are due to the small surface waves caused by the passage of the submerged body. For the case studied here, the surface wave effects were small compared to the convergence due to wake collapse.

Theory

The effects of the motion of a body through a fluid may conveniently be divided into two groups: short-period effects due to the flow field around the body, and long-period effects due to the persistent wake of the body. With body length 4·5 cm and speed 45 cm/sec, the short-period effects will have time constants in the neighbourhood of 0·1 sec. As will be seen below, internal waves in the density gradient of the experiment have much longer periods than this, and so very little energy may be expected to couple into the internal waves from the immediate flow field. Surface waves of length about 12 cm, and about 0·2 cm, propagate at 45 cm/sec, and some coupling of energy into the 12 cm wave may be expected, although since the top of the body is about 6 cm below the surface, the coupling will not be efficient.

For the wake, however, the situation is quite different. The forces on the tube of mixed fluid are precisely those which provide the restoring force in internal waves, so the wake should be an efficient generator of internal waves.

We shall employ the following notation: x_1 is the horizontal co-ordinate with origin on the centre line, x_2 the vertical co-ordinate with origin at the surface, increasing downward, ρ the density, ρ_0 the surface density, $\beta = +1/\rho(\partial\rho/\partial x_2)$ (cm^{-1}), ψ the stream function of internal waves ($\mathrm{cm}^2\,\mathrm{sec}^{-1}$), D, W the depth and width of fluid in the basin (cm), k_1, k_2 the horizontal and vertical radian wave-numbers of internal wave modes (cm^{-1}), n, m the horizontal and vertical mode numbers (dimensionless integers), ω the radian frequency of the internal wave mode (sec^{-1}); g is the acceleration due to gravity ($\mathrm{cm\,sec}^{-2}$), ξ the vorticity (sec^{-1}), ν the kinematic viscosity ($\mathrm{cm}^2\,\mathrm{sec}^{-1}$), D_1 the viscous dissipation in the body of the fluid per unit length ($\mathrm{cm}^4\,\mathrm{sec}^{-3}$), D_2 the viscous dissipation due to walls ($\mathrm{cm}^4\,\mathrm{sec}^{-3}$), E the energy content per unit length ($\mathrm{cm}^4\,\mathrm{sec}^{-2}$), χ a 'displacement function'

defined by $\partial\chi/\partial t = \psi\,(\mathrm{cm}^2)$, a the depth of the centre of the mixed fluid disturbance (cm), b_1 is half the horizontal width of the mixed fluid disturbance (cm), b_2 is half the vertical thickness of the mixed fluid disturbance (cm), Δ the lateral displacement at the surface (cm), G_{ij} the relative amplitude of a mode of horizontal order i and vertical order j (cm^2), and δ_{ij} the exponential time-decay rate of G_{ij} (sec^{-1}).

Internal waves are particularly simple to analyse for an exponential density gradient. A linear density gradient, if the total density range is small, closely approximates to an exponential gradient. In the present case, a linear gradient where the density never differs by more than $3\frac{1}{2}$ % from the mean, the assumption that the gradient is exponential will introduce very little error.

We therefore consider first a frictionless incompressible fluid with density described by

$$\rho = \rho_0 e^{+\beta x_2}. \tag{1}$$

m/n	$f\ (\mathrm{sec})^{-1}$
1	0·204
2	0·121
3	0·0834
4	0·0644
5	0·0510
∞	0
$\frac{1}{2}$	0·295
$\frac{1}{3}$	0·326
0	0·359

TABLE 1. Characteristic internal wave mode frequencies.

Because of the finite time of passage of the body, the flow régime will not quite be two-dimensional, but differences from two-dimensionality should be small enough that the greatly increased complexity of a three-dimensional treatment is not warranted.

It can readily be shown (cf. Lamb, 1932, § 235) that two-dimensional internal waves in a rectangular basin may be described by the stream function ψ where

$$\psi = A\, e^{-\frac{1}{2}\beta x_2} \sin k_1 x_1 \sin k_2 x_2 \sin \omega t. \tag{2}$$

Here A is a constant of dimensions $\mathrm{cm}^2\,\mathrm{sec}^{-1}$. If the finite rectangular basin has depth D and width W, we have the requirements

$$k_1 = n\pi/W, \quad k_2 = m\pi/D,$$

where n and m are integers. The characteristic equation then gives ω in terms of k_1 and k_2,

$$\left(\frac{g\beta}{\omega^2} - 1\right) k_1^2 = \tfrac{1}{4}\beta^2 + k_2^2. \tag{3}$$

In our experiment $\beta = 5{\cdot}2 \times 10^{-3}\,\mathrm{cm}^{-1}$, $k_1 = 0{\cdot}18n\,\mathrm{cm}^{-1}$, $k_2 = 0{\cdot}25m\,\mathrm{cm}^{-1}$, so that a sufficient approximation for equations (2) and (3) is

$$\psi \doteq A \sin k_1 x_1 \sin k_2 x_2 \sin \omega t, \tag{4}$$

and

$$\omega^2 = g\beta\{(k_2^2/k_1^2) + 1\}^{-1}$$
$$= 5{\cdot}1\,\mathrm{sec}^{-2}\{1{\cdot}96(m^2/n^2) + 1\}^{-1}. \tag{5}$$

Table 1 shows some internal-wave eigen-frequencies as a function of m/n.

Dissipation

The nature of the motion, with wave-numbers of the order of $1\,\mathrm{cm}^{-1}$ and viscosity of the order of $0{\cdot}02\,\mathrm{cm}^2\,\mathrm{sec}^{-1}$ gives time constants of the order of 50 sec, which are not negligibly long relative to the duration of the experiment, and so are worth closer examination. Energy dissipation from the wave motion can be expected from three sources: viscous dissipation in the body of the fluid, viscous drag on the walls and interaction with the turbulence in the wake. The first two may be approximately calculated in a straightforward fashion, but about the third little is known.

As to the first, it seems *a priori* reasonable to assume that the dissipation in the body of the fluid could be calculated on the assumption that the walls had no effect, and that wall effects could be separately treated. The validity of the assumption can then be examined *post hoc*.

With a cellular flow pattern, the viscous dissipation may be obtained in terms of the vorticity ξ and the kinematic viscosity ν (cf. Lamb, 1932, § 329). Thus for the body of the fluid, the time average of the dissipation (per unit length along the tank axis) will be given by†

$$\begin{aligned} D_1 &= \nu\int\int\overline{\xi^2}\,dx_1\,dx_2 \\ &= \nu\int\int\overline{(\nabla^2\psi)^2}\,dx_1\,dx_2 \\ &= \tfrac{1}{2}\nu(k_1^2+k_2^2)^2A^2\int\int\sin^2 k_1x_1\sin^2 k_2x_2\,dx_1\,dx_2 \\ &= \tfrac{1}{8}\nu(k_1^2+k_2^2)^2A^2WD. \end{aligned} \tag{6}$$

To calculate the effects of the walls, we shall assume that the wall influence penetrates only very slowly into the body of the fluid. Thus at small distances from the wall the flow will be the same as that which would obtain in the absence of the wall. The wall can then be regarded as a source of vorticity alternating at radian frequency ω.

The solution to this problem is also given, in essence, by Lamb (1932, § 345). If the velocity some distance from the wall is found to be $a\cos(\omega t+\epsilon)$ then the velocity at a (small) distance y from the wall will be given by

$$a\{\cos(\omega t+\epsilon)-e^{-\gamma y}\cos(\omega t-\gamma y+\epsilon)\}, \tag{7}$$

where

$$\gamma^2 = \omega/2\nu. \tag{8}$$

The average energy dissipation per unit wall area is thus $a^2(\omega\nu/8)^{\frac{1}{2}}$. Integrated over the three relevant surfaces (two sides and the bottom), this then amounts to

$$D_2 = A^2(\omega\nu/8)^{\frac{1}{2}}(k_1^2D+\tfrac{1}{2}k_2^2W). \tag{9}$$

The energy content, on the other hand, is

$$E = \tfrac{1}{8}(k_1^2+k_2^2)A^2WD.$$

Thus

$$D_1/E = \nu(k_1^2+k_2^2),$$

and

$$\frac{D_2}{E} = (8\omega\nu)^{\frac{1}{2}}\frac{\{(k_1^2/W)+(k_2^2/2D)\}}{(k_1^2+k_2^2)}.$$

† Kinematic units for energy and dissipation will be used throughout.

For $\nu = 0{\cdot}02\,\mathrm{cm^2\,sec^{-1}}$, which is the approximate value tabulated for this glycerin concentration, and a typical wave-number given by $m = n = 2$, we then find that $D_1/E = 0{\cdot}0078\,\mathrm{sec^{-1}}$, while $D_2/E = 0{\cdot}029\,\mathrm{sec^{-1}}$. For $m = 10$, $n = 2$, we have $D_1/E = 0{\cdot}13\,\mathrm{sec^{-1}}$, and $D_2/E = 0{\cdot}010\,\mathrm{sec^{-1}}$. Clearly, then, viscous dissipation at the wall is not of dominant importance (although not negligible) in the duration ($\sim 20\,\mathrm{sec}$) of our experiment, and dissipation in the body of the fluid is only very important in the higher modes.

The *post hoc* justification of our treatment of the wall resistance is as follows. A typical value of ω is about $1\,\mathrm{sec^{-1}}$, with values ranging between twice and half this figure. The 'skin thickness' $(2\nu/\omega)^{\frac{1}{2}}$ is then about 2 mm which is two orders of magnitude smaller than the tank dimensions. It might be argued that the concentration of the loss at the wall would distort the internal wave grossly. However, the motion of each mode represents alternation of the concentration of energy between kinetic and potential energy. The transfer from potential energy to kinetic is through the pressure field, which is an extensive force. The energy loss is thus distributed throughout the fluid, provided that the relative loss per cycle is small, as is the case here.

Excitation of modes

The details of mode excitation are difficult to follow with a theory, since the formation of a tube of mixed fluid and the initial collapse of this tube will occur simultaneously. However, an idealized model may reproduce the main features.

Provided that the tube of mixed fluid is formed rapidly compared with the characteristic time scales of the internal waves (i.e. with $(g\beta)^{-\frac{1}{2}} \sim 0{\cdot}4\,\mathrm{sec}$) the response should approximate that due to an initial localized displacement with an initially zero velocity. In fact 0·4 sec is *not* a long time compared with that required to form the wake, but a rough analysis based on this assumption is nevertheless indicative.

The effective displacement must be zero at the axis of the wake, co-ordinates $(0, a)$. A simple representation of such a displacement can be obtained as follows. Let us define a function $\chi(x_1, x_2, t)$, where $\partial\chi/\partial t = \psi$, ψ being a stream function. Now let us take

$$\chi = Gx_1(x_2 - a)\exp\left[-\{x_1^2 b_1^{-2} + (x_2 - a)^2 b_2^{-2}\}\right], \tag{10}$$

which represents a disturbance of horizontal scale b_1, vertical scale b_2 centred about $(0, a)$. A system of image disturbances, imaged in the walls and the surface, should in principle be included, but if b_1 and b_2 are small compared with the tank dimensions the images may be neglected with little effect. We may now examine the excited modes by expanding χ in a series of terms of the form (4), i.e.

$$\chi = \Sigma\Sigma B_{ij} \sin k_i x_1 \sin k_j x_2 \cos \omega_{ij} t. \tag{11}$$

At time $t = 0$, equating (10) and (11) permits calculation of the B_{ij}. Thus we have

$$B_{ij} = \frac{2G}{WD}\int_0^D \int_0^W x_1(x_2 - a)\exp -\{x_1^2 b_1^{-2} + (x_2 - a)^2 b_2^{-2}\} \sin k_i x_1 \sin k_j x_2\, dx_1\, dx_2. \tag{12}$$

If n is odd, this yields zero. If n is even, and $b_1; b_2 \ll W; D$ it gives

$$B_{ij} = \tfrac{1}{8}\pi b_1^3 b_2^3 k_i k_j (G/WD) \exp -\tfrac{1}{4}\{k_i^2 b_1^2 + k_j^2 b_2^2\} \cos k_j a.$$

In our case $a = 7{\cdot}5$ cm. Since the theoretical model is far from exact, it is difficult to assign a value for b_1, b_2 with any precision, but $b = 1{\cdot}5$ cm corresponds to a maximum value of χ at a position about 1·1 cm from the wake axis. This is the radius of the motor, and also seems reasonable in view of the results shown in figure 3.

We define

$$G_{ij} = k_i k_j \exp -\tfrac{1}{4}\{k_i^2 b_1^2 + k_j^2 b_2^2\} \cos k_j a. \tag{13}$$

Some representative values are in given table 2, taking $b_1 = b_2 = 1{\cdot}5$ cm.

n	m	G_{ij} (arbitrary units)	δ_{ij} (sec^{-1})
2	1	−0·025	0·016
2	2	−0·084	0·014
2	3	0·146	0·015
2	4	0·065	0·019
2	5	−0·184	0·022
2	6	0·037	0·030
2	7	0·091	0·038
2	8	−0·046	0·046
2	9	−0·016	0·057
2	10	0·025	0·068
4	2	−0·135	0·025
4	4	−0·105	0·026
4	10	0·041	0·073
6	2	−0·142	0·033
6	4	0·110	0·035
6	10	0·042	0·081

TABLE 2. Relative amplitude and decay rates for internal wave modes.

Clearly, with so many modes activated and with no harmonic relation among the mode frequencies, the resulting motion will be most complex. The surface dye spots, whose motion is shown in figure 5, are well situated to respond to many modes.

The behaviours shown in figures 4 and 5 are from four flow realizations with all experimental parameters as nearly equal as we could make them. It is evident that the behaviours are different. We must therefore infer that some statistical variation in internal wave excitation must occur. The fact that the exciting phenomenon is a turbulent one means that this statistical behaviour does not cause surprise. The best we can hope to do theoretically, then, is to show that the motions observed are each consistent with a reasonable distribution of mode excitation. (Of course a *statistical* theory might be attempted, but this should be compared with statistical observations—which we do not have.)

We have calculated the damped motion of some 30 modes. More could, of course, be computed. However, to fit the observations by the best selection from these modes would be 'empiricism' of the worst kind, and we shall not attempt it.

Instead we have grouped all modes with the same horizontal wave-number, assuming that they are activated in the manner given in equation (12). The observations we have for comparison are of two kinds; the collapse of the wake and the relative displacement of the surface dye spots. Our computations have thus been made of quantities directly relatable to these observations.

Under a linearizing assumption, the displacement of a surface particle is given by

$$\Delta = -\partial x/\partial x_2 \quad \text{at} \quad x_2 = 0,$$
$$= Q\Sigma k_j G_{ij} \sin k_i x_1 \cos \omega t\, e^{-\delta_{ij} t}, \tag{14}$$

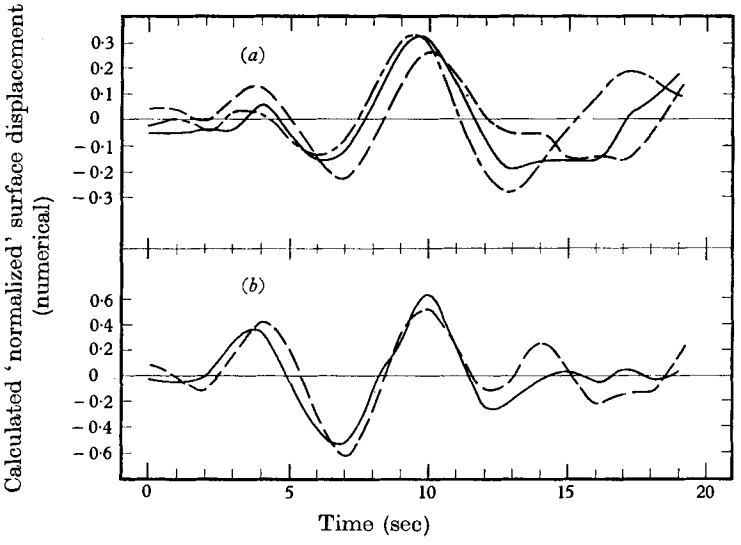

FIGURE 6. (*a*) Calculated influence of depth of disturbance (*a*) on surface displacement due to modes $n = 2$, with half vertical thickness of disturbance $b_2 = 1{\cdot}5$ cm, as a function of time, $\nu = 0{\cdot}02$ cm^2 sec^{-1}: $a = 7{\cdot}0$ cm – – –, $a = 7{\cdot}5$ cm ——, $a = 8{\cdot}0$ — — —. (*b*) Similar to figure 6 (*a*) except $b_2 = 2{\cdot}5$ cm and $a = 8$ cm omitted. $a = 7{\cdot}0$ cm – – –, $a = 7{\cdot}5$ cm ——.

where Q is an amplitude factor and the δ_{ij} are characteristic decay-time constants calculated on the basis of viscous decay as discussed above. In order to show the variety of possible results, we have computed

$$\sum_{j=1}^{10} k_i G_{ij} \cos \omega t\, e^{-\delta_{ij} t}$$

for times up to 19 sec, and some range of the available parameters. The results are displayed in figures 6 and 7.

Figure 6 (*a*) shows the effect, on modes $n = 2$, of varying only the depth of the centre of the disturbance, with b_2 held constant at 1·5 cm. The curves are 'normalized' in such a way that if all the modes were in phase and at peak amplitude at time $t = 0$, the resulting amplitude would be unity. It can be seen that there is little variation in the apparent frequency of the phenomenon, but rather large detailed differences because of variations in the relative excitation of different modes. It will be noted that the solid curve ($a = 7{\cdot}5$ cm) corresponds rather well to the observations of run IV, in figure 5 (*c*), but none is in particularly good agreement with those of run III in figure 5 (*a*) and (*b*).

Figure 6 (*b*), when compared with 6 (*a*), shows the effect of increasing the vertical scale of the disturbance. Increasing this vertical scale (increasing b_2), as can be seen from equation (13), reduces the relative excitation of modes with larger values of k_j (or m). This results in somewhat higher apparent frequency. Run III in figure 5 (*a*) and (*b*) seems more nearly of this character.

Figure 7 (*a*) displays the results for three values of horizontal wave-number, corresponding to $n = 2$, 4 and 6. The increase of apparent frequency as this wave-number increases is evident. Comparison with the observations shown in figure 5 shows that high horizontal wave-numbers cannot dominate because their frequency is too high.

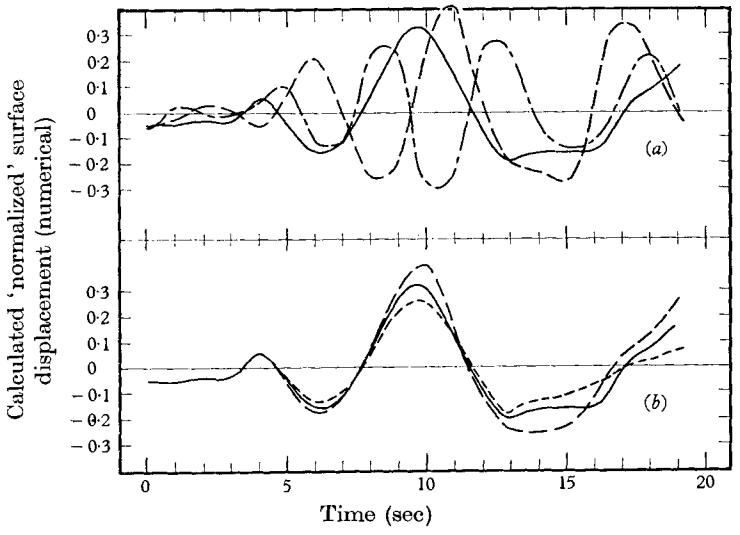

FIGURE 7. (*a*) Calculated influence of the order of horizontal wave-number on the behaviour of surface displacement as a function of time. $a = 7{\cdot}5$ cm, $b_2 = 1{\cdot}5$ cm, $\nu = 0{\cdot}02$ cm^2 sec^{-1}. $n = 2$ ——, $n = 4$ – – –, $n = 6$ — — —. (*b*) Calculated influence of assuming different values for the viscosity on the behaviour of surface displacement as a function of time. $n = 2$, $a = 7{\cdot}5$ cm, $b_2 = 1{\cdot}5$ cm. $\nu = 0$ cm^2 sec^{-1} — — —, $\nu = 0{\cdot}02$ cm^2 sec^{-1} – – –, $\nu = 0{\cdot}04$ cm^2 sec^{-1} ——.

In figure 7 (*b*), to demonstrate the dissipation effects, we have plotted curves for $\nu = 0$, for $\nu = 0{\cdot}02\,\text{cm}^2\,\text{sec}^{-1}$ (the tabulated value for a glycerin solution of about the concentration used here), and for $\nu = 0{\cdot}04\,\text{cm}^2\,\text{sec}^{-1}$.†

It appears that the assumption that dissipation is purely viscous does not lead to an appreciable underestimate of the observed damping. Thus turbulence cannot be a dominant contributor to decay—neither residual turbulence in the wake nor any turbulence induced by the internal wave motion.

The comparison between the calculations shown in figures 6 and 7 and the observations of figure 5 lead us to believe that although we are unable to produce exact correspondence between calculation and observation, the motion of

† The figures for this last curve were available, we must admit, because we at first made the common undergraduate error of using the *energy* dissipation correction for the *amplitudes*.

surface dye spots is chiefly due to modes with $n = 2$. This is borne out by closer examination.

The dye spots of run III, whose separation is shown in figure 5 (*b*), are rather close to the centre line. The relative response to modes with larger values of n is therefore rather greater than to the lower wave-numbers. For $n = 2$; 4; 6 the ratios are 1:1·49:1·64.

On the other hand, comparison with the theoretical curves of figure 7 (*b*) reveals that the similarity between the observations and the calculated curves for $n = 2$, particularly the one using $\nu = 0{\cdot}02\,\mathrm{cm^2\,sec^{-1}}$, is quite striking. This is especially true if a virtual origin, 2 sec after passage, is used for the time. No such agreement is observed for the modes with larger values of n. The apparent frequency characteristic of these modes is too great. It will also be noted that the observations of run IV fit better with the calculations shown in figure 7 (*b*), for $b_2 = 1{\cdot}5\,\mathrm{cm}$, than with those of figure 6 (*b*), with $b_2 = 2{\cdot}5\,\mathrm{cm}$. The difference between the two calculations arises because with the larger value of b_2 there is very little excitation of modes $m > 5$, while for the smaller value of b_2 modes up to $m = 10$ remain important.

The movement of surface dye spots thus leads us to believe that while a large number of vertical modes (different values of m) are excited in this flow realization, the chief horizontal modes (different values of n) contributing are those with $n = 2$.

The results for the other flow realization may be contrasted. The two wider-spaced dye spots (figure 5 (*a*)) respond to modes $n = 2$; 4; 6 in the ratio $1:0{\cdot}08:-0{\cdot}95$; the more closely spaced spots (figure 5 (*b*)) in the ratio 0·59:0·95:0·99. (These numbers may also be used in comparison with the wider spaced spots.)

If modes with $n > 2$ are important, then, we should expect large differences between the behaviour shown in figure 5 (*a*) and (*b*). There *is* a difference, but it is the similarity rather than the difference which is the notable feature of the curves. Indeed, if we assume that *only* the modes $n = 2$ are activated, the curve shown in figure 5 (*b*) would be identical with that of 5 (*a*) except that the amplitude would be only 0·59 as large. We have therefore shown, dashed, such a curve on figure 5 (*b*). Evidently most of the features are due to the modes $n = 2$, and less than half the amplitude is due to high modes.

All this means that in both runs there must be a very striking difference in the effective horizontal and vertical scales of the disturbance. Mode $n = 2$ has a horizontal wave-number of $0{\cdot}18\,\mathrm{cm^{-1}}$. However, the mode with the largest contribution to figure 6 (*a*) (and to figure 7 (*b*)) has a vertical wave-number $1{\cdot}25\,\mathrm{cm^{-1}}$, nearly an order of magnitude larger! It appears that the density gradient not only causes the wake to collapse, but also exhibits its well-known inhibiting effect on vertical motions, causing the turbulence to be much more effective in mixing horizontally than vertically.

We have, moreover, additional information—the behaviour of the collapsing wake. Since the top of the wake is approximately in the centre of the tank, in our model this wake edge may be fairly well represented by the displacement

$$\partial x/\partial x_1, \quad \text{at} \quad x_2 = \tfrac{1}{2}D \quad (x_1 = 0),$$

i.e. by $$Q\sum_{ij} k_i\,|G_{ij}|\cos\omega t\, e^{-\delta_{ij}t}, \tag{15}$$

where j is even and i is *odd*.

Once more we sum over modes with the same value of n, and for two values of b_2. The results are displayed in figure 8, normalized to unity at time zero. Before examining the rate of wake collapse, it is necessary to consider carefully the relation between the computed curves and the observations. By fitting the experimental and calculated curves, the following instructive quantitative calculation may be made.

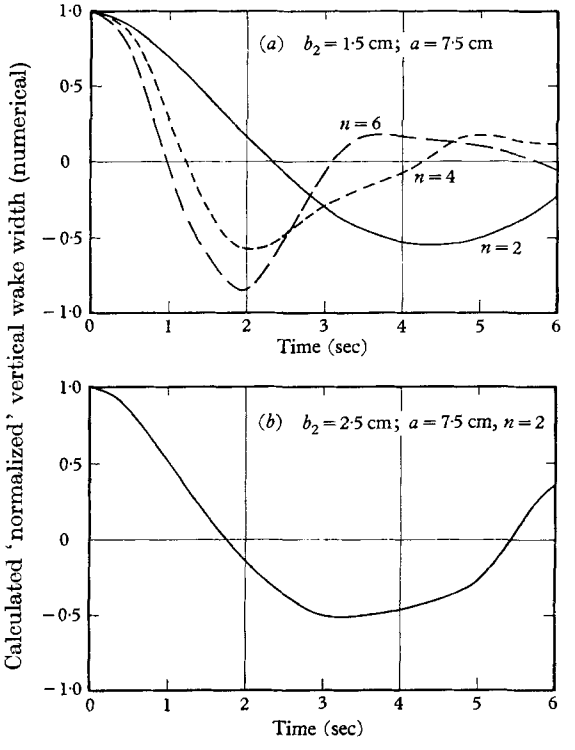

FIGURE 8. (*a*) Calculated displacement at tank centre $(0, \frac{1}{2}D)$ as a function of time, with different values of horizontal wave-number and $b_2 = 1{\cdot}5$ cm. (*b*) Similar to figure 8(*a*) for $b_2 = 2{\cdot}5$ cm and $n = 2$.

The peak increase in spot separation shown in figure 5 (*c*) is about 0·8 cm. If the motion is entirely due to modes for which $n = 2$, it is a simple calculation to show that the maximum displacement of a surface particle would be 0·9 cm. On the other hand, the peak value of $\Sigma k_i G_{2j}$ for $n = 2$, $b_2 = 1{\cdot}5$ cm, is 0·26 cm. The relevant amplitude factor Q is thus about 3·5. We may then compute the corresponding initial displacement at the tank centre, which is therefore given by $3{\cdot}5 \times 0{\cdot}25\Sigma\,|G_{2j}|$ (j odd) and turns out to be 0·6 cm. Elimination of this much displacement above and below the wake leads to a reduction in thickness of 1·2 cm—which is more than the observed collapse! We must conclude that some of the initial wake collapse occurs before the maximum wake growth has been completed.

This makes difficult comparison between the observations of figure 4 and the calculations shown in figure 8. Nevertheless, it does seem that the observations indicate a faster collapse than we should expect from modes $n = 2$. Some contribution from higher horizontal modes is thus likely. It should be noted that because of the factor k_i in equation (15), modes with higher values of n are appreciably more effective in the vertical movements of the wake collapse than in the horizontal dye spot movements.

Perhaps some admixture of effects from modes of different horizontal wave-number accounts for the absence in the observational data of the 'overshoot' and 'rebound' so noticeable in the calculated curves of figure 8.

Summary and conclusions

It has been shown that the turbulent wake behind a self-propelled body behaves quite differently when the fluid is stratified from when it is homogeneous. In the stratified case the tube of fluid mixed by the turbulence of the wake is subject to buoyancy forces, and tends to collapse vertically.

This vertical collapse is shown to be an efficient generator of internal waves which reveal themselves in movements at the surface. It appears that while internal waves with high vertical wave-numbers are excited (indeed we know of no mechanism reported in the literature so efficient in producing high mode excitation) only modes with rather low horizontal wave-numbers contain much energy. This leads us to believe that the effective initial disturbance is much wider than it is deep—due perhaps to the inhibition on vertical turbulent mixing imposed by the density gradient.

Since the observed rate of decay of the induced motion does not appreciably exceed that calculated to arise due to viscosity alone, we infer that turbulence is not of much importance, in this case, in the energy dissipation.

We wish to thank Dr H. L. Grant for valuable collaboration in performing the experiments, and Dr J. Uretsky for useful ideas on the theoretical understanding.

REFERENCE

LAMB, H. 1932 *Hydrodynamics* (6th edition). Cambridge University Press.

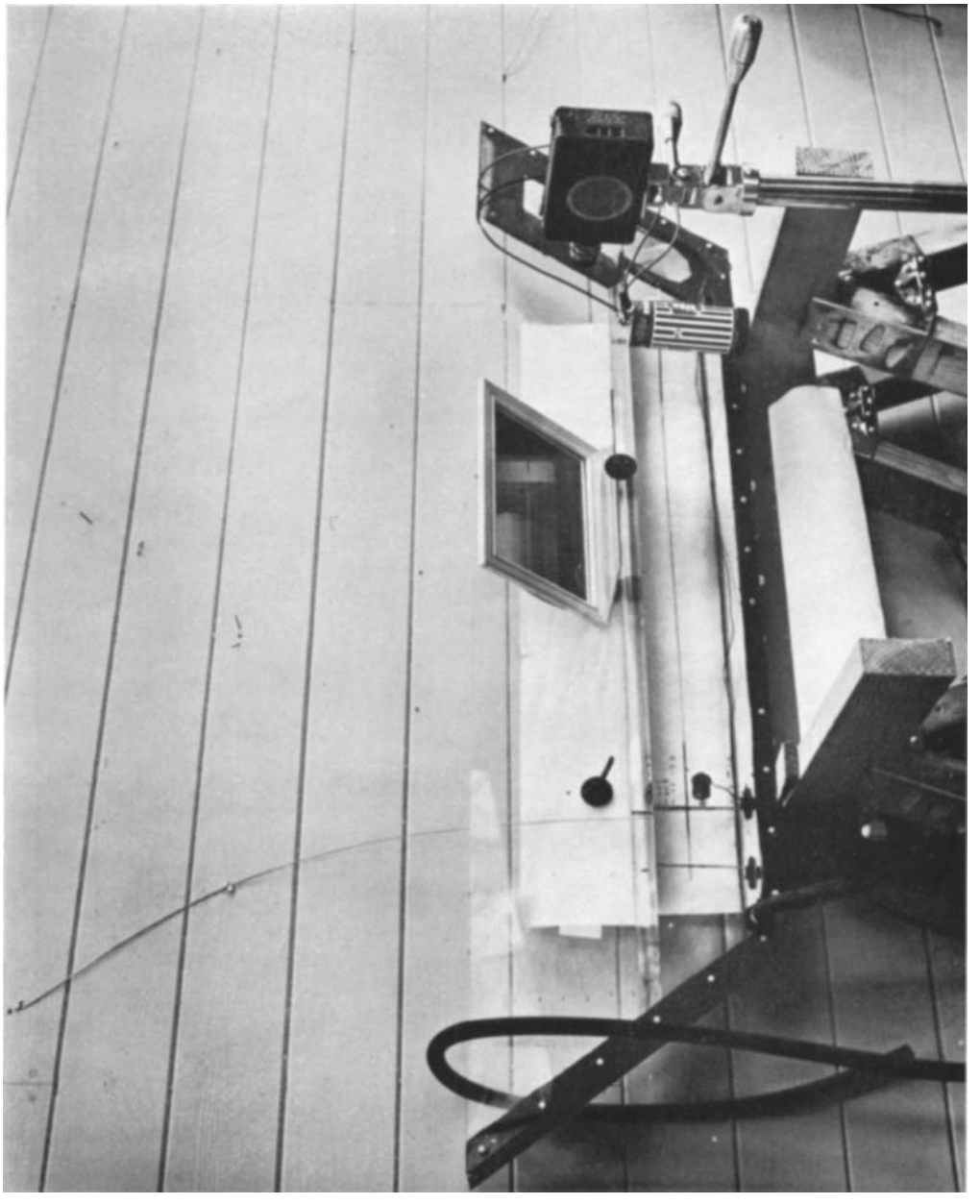

FIGURE 1. Experimental apparatus.

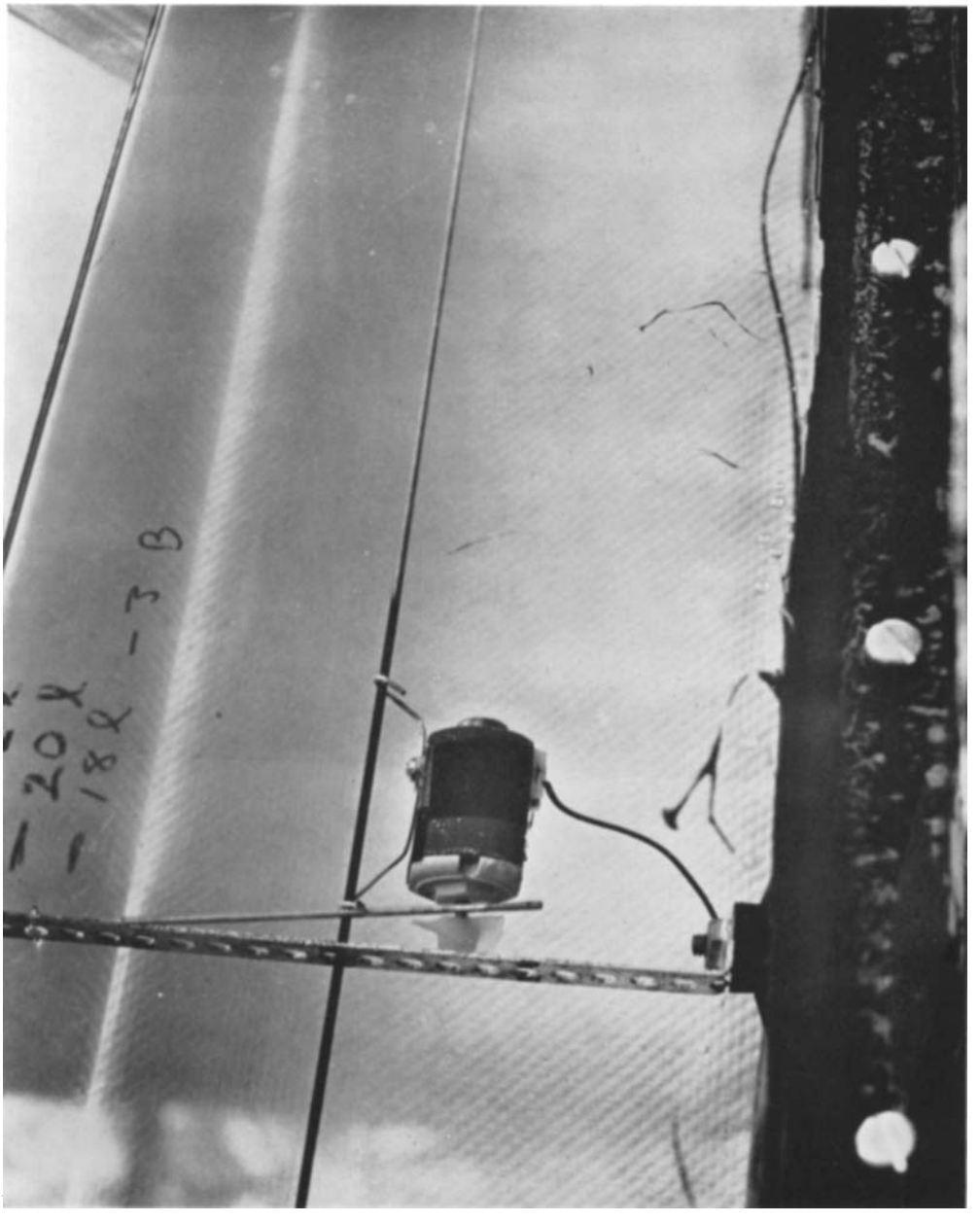

FIGURE 2. Self-propelled body.

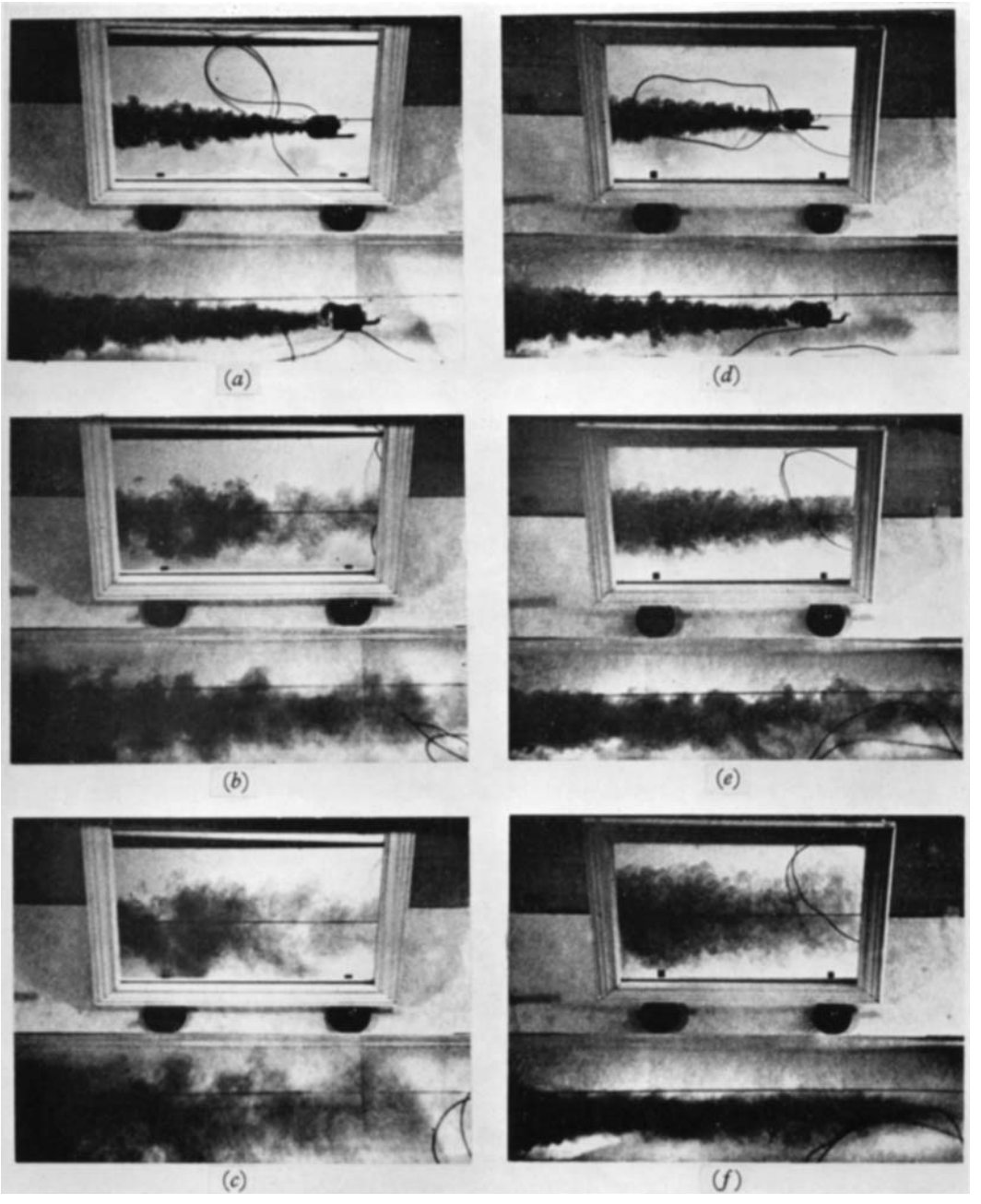

FIGURE 3. Horizontal (in mirror above) and vertical wakes. (*a*), (*b*) and (*c*), no density gradient at time equal to 0, 1 and 3 sec respectively; (*d*), (*e*) and (*f*), density gradient at time equal to 0, 1 and 3 sec respectively.